We are IntechOpen,
the world's leading publisher of
Open Access books
Built by scientists, for scientists

6,900
Open access books available

186,000
International authors and editors

200M
Downloads

154
Countries delivered to

Our authors are among the

TOP 1%
most cited scientists

12.2%
Contributors from top 500 universities

CLARIVATE ANALYTICS
BOOK CITATION INDEX
INDEXED

WEB OF SCIENCE™

Selection of our books indexed in the Book Citation Index
in Web of Science™ Core Collection (BKCI)

Interested in publishing with us?
Contact book.department@intechopen.com

Numbers displayed above are based on latest data collected.
For more information visit www.intechopen.com

CW THz Wave Generation System
with Diode Laser Pumping

Srinivasa Ragam
Lehigh University, Department of ECE, Bethlehem,
USA

1. Introduction

This chapter contains the work of continuous-wave (CW) terahertz (THz) radiation; the THz waveform generation, propagation and detection. THz technology attracts increasing interest due to its versatile application possibilities in medical imaging, spectroscopy, THz communication, nondestructive screening, and identification of many chemical elements. For such applications, it is necessary to realize compact and cost-efficient THz sources, which emit a broadband spectrum on the one hand, and can be tuned in frequency with a narrow linewidth on the other hand. Thus, the realization of a compact, cost-efficient and frequency-tunable CW THz radiation source was presented in this chapter. The principle of THz wave generation is by exciting the phonon- polariton in bulk GaP crystal on the basis of nonlinear optical method. The theoretical concept of difference frequency generation (DFG) on the basis of non-linear optics is well known. The generation of widely tunable CW single-frequency THz waves from GaP based on laser diode (LD) pumping is described in this chapter. DFG method is a parametric process based on second-order nonlinearities has recently been proved to be one of the most promising techniques for the efficient generation of widely tunable, monochromatic, high-power and coherent THz wave with a suitable combination of light sources and nonlinear optical (NLO) crystals. The region of the electromagnetic spectrum from 0.1 THz to 10 THz is very attractive because THz waves have a variety of applications in several fields. In 1963, Nishizawa [1], [2] proposed the generation of THz waves via resonance of phonons and molecular vibrations in compound semiconductors, following the realization of a GaP semiconductor laser [3], [4]. An electromagnetic wave with a frequency of 12.1 THz was generated from GaAs pumped by a GaP Raman laser at a power of 3W [5]. Our group succeeded in generating wide frequency-tunable high power THz wave signals from GaP with Q-switched pulse pumping [6]. Also, time domain THz sources have been developed based on femto-second pulsed lasers [7-10]. Compared to pulsed THz sources, continuous-wave (CW) THz sources provide a THz spectrum with a narrower line width and a higher spectral THz power [11, 12]. The potential applications of CW THz waves include high resolution THz spectroscopy, multi-channel telecommunications and imaging technologies [13-19]. Several CW THz wave sources such as, Gunn diodes, TUNNETT diodes, backward wave oscillators, CO_2-laser pumped gas lasers, sources based on nonlinear optical difference frequency generation(DFG) [20], optical parametric oscillators [21], free-electron lasers, quantum cascade lasers [13,14] and photo mixers [15-16] have been developed.

Broadband tunability and power levels of at least tens of microwatt are highly desirable for CW THz spectroscopy. In addition, it is also desirable that the THz source is compact, cost-efficient and operating at room temperature. Some CW THz sources listed above can deliver sufficient power. However, either they are bulky, expensive and/or have a limited frequency tunability. CW THz sources that are compact and tunable throughout the frequency range from 100 GHz to 10 THz with tens of microwatt power levels still remain a technological challenge. A simple configuration of THz sources even is desired for easy maintenance of the devices. Moreover, the stability of THz radiation is a requirement for reliable measurements. Pumping with narrow linewidth diode lasers in nonlinear optical method of DFG will enable the generation of narrow linewidth CW THz waves of a MHz order. Semiconductor lasers are stable at light intensities, and spectrometers using CW THz waves do not need prolonged measurements with much repetition. With this motivation, we had successfully generated tunable CW THz waves from GaP crystal with diode laser pumping in the frequency range of 0.69 - 2.74 THz [22]. However the output power was limited to in the order of pW in that configuration. By using a two fiber amplifier system for amplifying the optical power of input diode lasers, we have reported that the output power of THz waves was improved nW order with employing a 20 mm long GaP [23]. In addition, the frequency of THz wave was tuned up to 4.42 THz in that configuration.

2. CW THz wave generation emission system with diode laser pumping using GaP crystal

Semiconductor NLO crystals with birefringence, such as $ZnGeP_2$ and GaSe, have been widely used as DFG crystals for THz generation due to their exotic nonlinear optical properties in the THz region [24, 25]. When the process of difference frequency mixing is phase matched using birefringence, a coherent and powerful THz wave will be obtained. Zinc blende semiconductor crystals, such as GaP is an excellent candidate for the generation of the THz radiation via difference frequency mixing. These crystals have relatively high damage threshold compared with organic crystals and can be grown with high purity and large size. Especially, their second-order nonlinear susceptibilities, $\chi^{(2)}$, are one or two orders of magnitude larger than those of typical second-order nonlinear materials such as $LiNbO_3$ and KTP [26, 27]. Furthermore, their absorption coefficient in the THz region is several times smaller than that of $LiNbO_3$ [28]. It is well known that, in the anisotropic birefringent crystals, the input pump and signal waves, λ_p and λ_s, for difference frequency mixing, and the generated THz wave, λ_T, are generally all in the same transmission window of the nonlinear crystal. In other words, their corresponding refractive indices all belong to the same dispersion curve. The dispersion is negative for three interactive waves, that is,

$$\frac{n_T - n_{p,s}}{\lambda_T - \lambda_{p,s}} < 0 \; ; \; (\lambda_p < \lambda_s < \lambda_T) \tag{1}$$

Where n_k is the refractive index at the wavelength λ_k ($k = p$, s, T). It is easy to satisfy the phase-matching conditions for DFG based on the normal dispersion property of nonlinear crystals and birefringence phase-matching technique. As for optically isotropic materials, such as GaP doesn't possess any birefringence. Fig. 1 shows the dispersion relation for the GaP crystal, which are generated according to its Sellmeier equation [29]. For the case of

THz-wave generation using DFG technique, the interacting pump and signal sources are generally in the NIR transmission window of the nonlinear crystal (curve with blue color as shown in Fig. 1), while the generated THz wave is in the FIR transmission window (curve with red color as shown in Fig. 1), on the other side of the crystal's Reststrahlen band, corresponding to the larger refractive indices. In the process of THz-wave DFG, the energy conservation condition is well known and is given by

$$\frac{1}{\lambda_p} - \frac{1}{\lambda_s} = \frac{1}{\lambda_T} \tag{2}$$

and the momentum conservation condition is given as

$$k_p - k_s = k_T, \quad \text{or} \quad \frac{n_p}{\lambda_p} - \frac{n_s}{\lambda_s} = \frac{n_T}{\lambda_T} \tag{3}$$

On the basis of DFG, continuous-wave (CW) THz wave generation is possible from GaP by pumping with laser diodes. We demonstrated the generation of a narrow line width, higher power, and wide frequency tunable THz waves using various GaP crystals and NIR beam spot sizes. It is known that the frequency resolution and the power stability of the THz waves are determined by the input lasers line width and power stability.
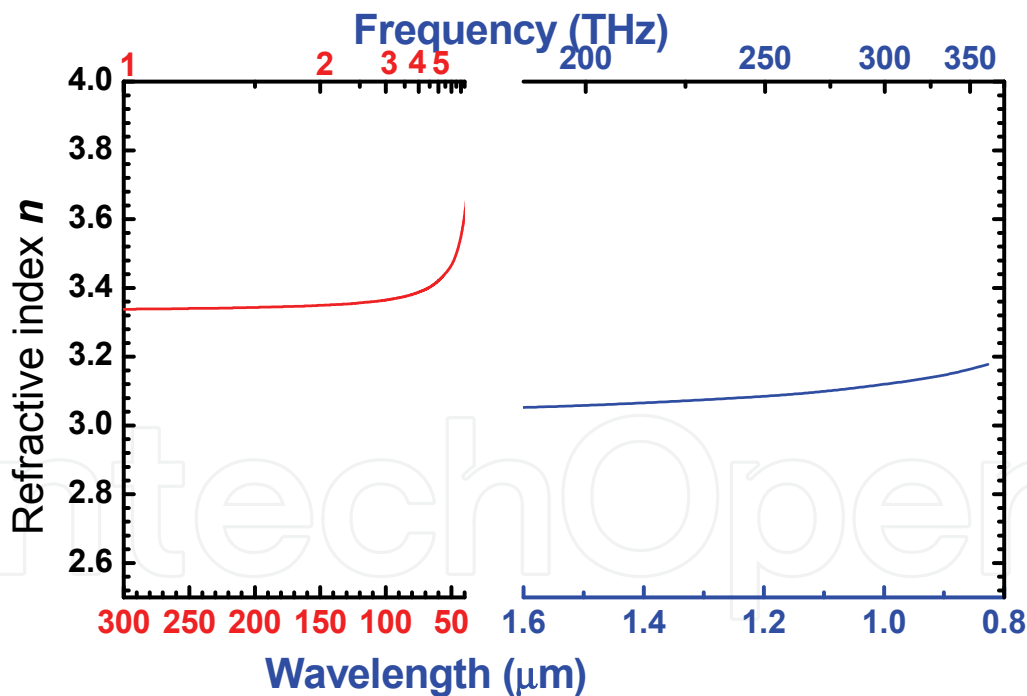

Fig. 1. Dispersion relation of GaP.

The advantages of laser diodes are: narrow line width of a few MHz, wide frequency tunability with stable output power and hence we chosen a distributed feedback (DFB) laser and an external cavity laser diode (ECLD) as pump and signal lasers. It is well known that the output power of the generated THz waves in difference frequency generation (DFG) is related to the input laser powers as follows [30]

$$P_{THz} = A\left(\frac{P_1 P_2}{S}\right)L_{eff}^2 \tag{4}$$

where P_1, P_2 are the effective powers of the pump and signal beams. L is the effective interaction length of the two near-IR beams inside the crystal (GaP), and S is the cross-sectional area of the pump and signal beams defined by the $1/e^2$ radius of the Gaussian beam, and A is a material constant for generating THz waves. From above equation (4), it is known that THz power scaling can be possible by (i) increasing the pump and signal powers P_1, P_2. (ii) proportional to the square of crystal length (iii) inverse proportional to the pump beam cross-sectional area, S. Hence we used two Yb doped fiber amplifiers (FAs) to amplify the output power of each laser diode as shown in the fig. 2(a).We studied the THz output power relation with various lengths of GaP crystals over a wide frequency range and also the THz power dependence with beam spot size of pump and signal lasers

3. Experimental method

The experimental set up for CW THz wave generation is shown in the Fig. 2(a). The pump and signal lasers are DFB laser and an ECLD respectively.
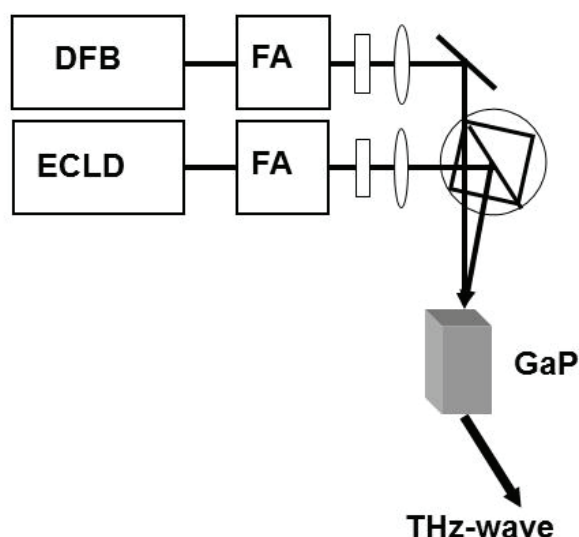

Fig. 2. (a) Schematic of the experimental set up used for generation of CW THz waves in GaP crystal.

The wavelength of DFB laser is automatically tuned from 1058 -1061 nm with a line width of 2 MHz by changing the temperature of the diode. The wavelength of ECLD can be manually tuned from 1020 nm to 1080 nm with a line width of 2MHz. Polarization maintained (PM) ytterbium-doped two Fiber amplifiers (FAs) are used to separately amplify the output power of each laser diode up to 2 W. The amplified laser beam from each FA is collimated to a diameter of 3 mm with a circular shape by using micro lenses of focal length 8.5 mm. A very small angle between the two beams is needed for DFG to satisfy non-collinear phase matching condition. So finally the collimated beams from each FA are combined on a cubic polarizer, which is mounted on a linear and rotating stage platform. An efficient spatial overlap of NIR laser beams is automatically realized on the input surface of a GaP crystal at any angle of the beams by adjusting the translation movement of the beam combiner. To

investigate the THz wave power dependence on GaP crystal length, we used 2.5mm, 5 mm, 10mm, 15 mm, 20 mm long and 3 mm thick undoped semi-insulating GaP crystals in the experiment. The GaP is cut into a rectangular shape of length in <110> direction and thickness in <001> direction.
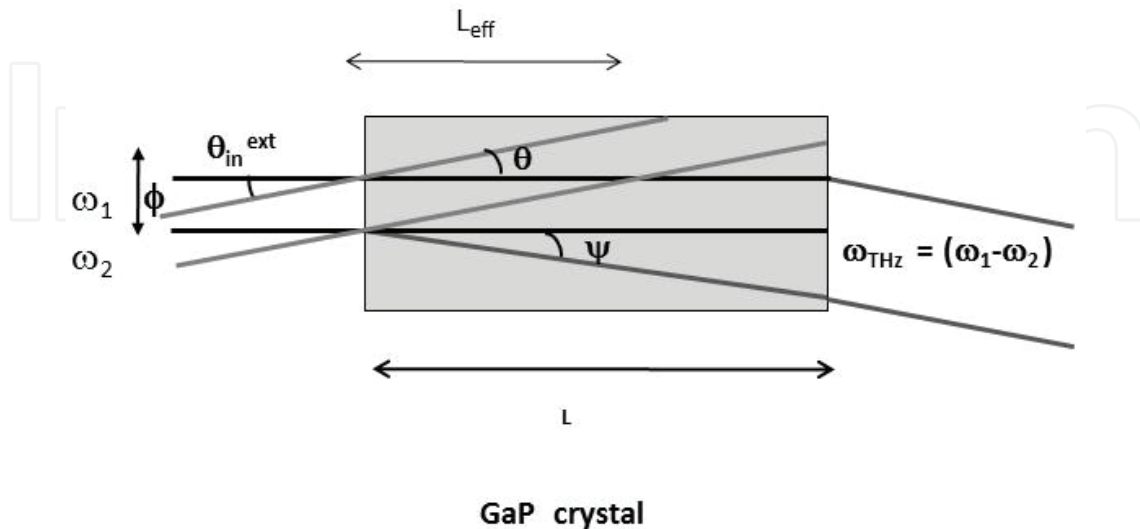

GaP crystal

Fig. 2. (b) Typical GaP crystal cut for non-collinear phase-matched DFG.

Both the input and output faces of crystal are coated with Al_2O_3 using EB- evaporation (JEOL) after mechanical polishing and chemical etching. The polarizations of the pump and signal beams are adjusted in <001> and <110> directions respectively. The line-width of each laser is measured to be 2 MHz using a fabry-perot etalon. The generated CW THz waves are either collected by a polyethylene (PE) lens or with parabolic mirrors and detected with a Si Bolometer, cooled at 4.2 K. The Si bolometer is placed in the direction of the generated THz waves, which leave the GaP crystal output face at 40o- 45o to the surface normal. Black polyethylene film is used to filter out near IR radiation. The THz signal is measured with lock-in-amplifier.

4. Results and discussion

Figure 2(b) shows typical GaP crystal cut for non-collinear phase matched DFG at $\omega_{THz} = \omega_1-\omega_2$ where ω_1,ω_2 are frequencies of ECLD and DFB lasers respectively. The ω_1 beam incident along normal to the input face and ω_2 beam is incident at an external angle θ_{in}^{ext} so that the angle between two input beams inside the GaP crystal is

$$\theta = sin^{-1}\left(\frac{1}{n}sin\theta_{in}^{ext}\right) \qquad (5)$$

Where n = 3.105 is the refractive index at the frequency, ω_2. Under phase matched conditions, the ω_{THz} propagates at an angle (ψ) relative to the ω_1 beam as shown in fig. 2(b). The critical angle for total internal reflection ~ 17. 4° in GaP. We generated THz waves over a wide frequency range from 0.69 – 4.42 THz as θ_{in}^{ext} is varied from 8′ to 45′. Figure 3 shows the phase-matching angle (θ_{in}^{ext}) dependence of the THz wave output power at various THz frequencies, where θ_{in}^{ext} is angle between the two lasers outside the GaP crystal. THz waves

are generated over a wide range from 1.4 THz – 4.42 THz as θ_{in} ^{ext} is varied from 8′ to 45′. In this measurement, the GaP crystal is 10 mm long and the pump beam is incident nearly normal to the crystal surface. The linewidth of THz wave is estimated to be 4 MHz. The combined beam spot size of lasers on the GaP surface is 700μm and polyethylene lens is used to collect the emitted THz waves.
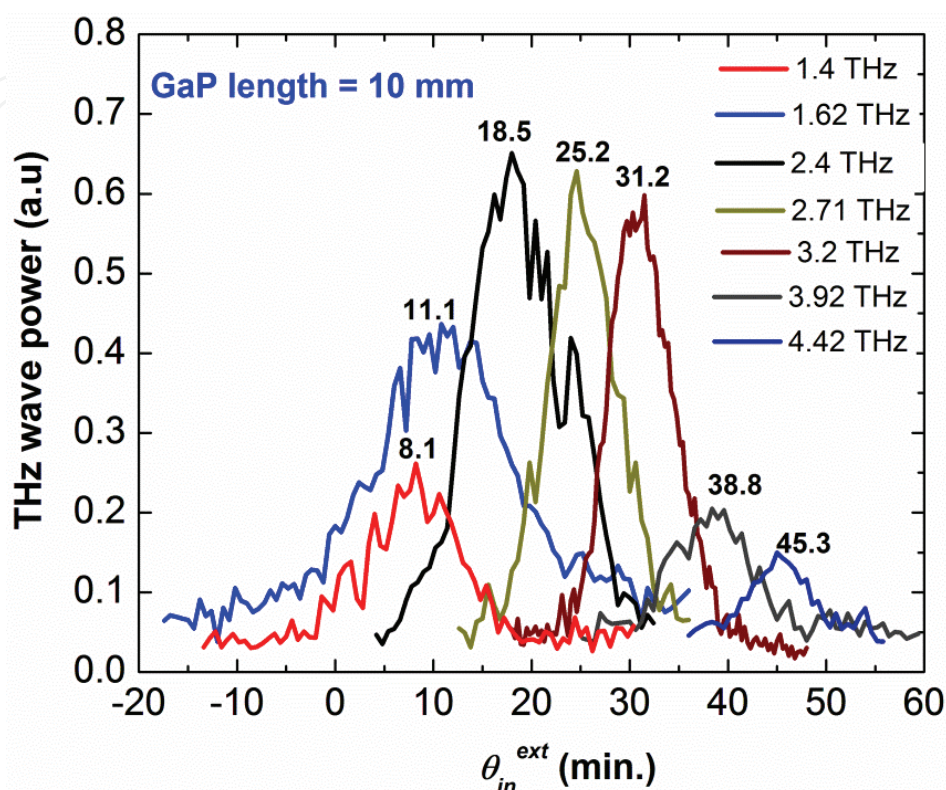

Fig. 3. The phase-matching angle $\left(\theta_{in}^{ext}\right)$ dependence of the THz wave output power at various THz frequencies, where θ_{in}^{ext} is angle between the two lasers outside the GaP crystal.

Fig. 4 shows the phase matching angle relation with THz wave frequency. The slope of the experimental data is 0.154/ THz = 2.67 mrad/ THz while slope of the solid curve is calculated as 2.91 mrad/THz. The experimental data agrees with the theoretical value, which is the θ_{in} ^{ext} curve as a function of THz wave frequency for phonon-polariton branch of GaP. Increasing θ_{in} ^{ext} shifted the generated THz wave frequencies slightly higher, similar to the result of pulse pumping. A continuously frequency tunable from 1.4- 4.42 THz can be generated in GaP crystal by sweeping the wavelength of the pump laser. Fig. 5 shows the frequency dependence of THz wave maximum power. It is seen that the THz wave power increases rapidly from 1.4 – 2.1 THz as the θ_{in} ^{ext} is varying from 8-16.2′. The THz wave maximum power is remained over a frequency range 2.1 – 3.2 THz.

In the lower frequency (below 2 THz) the free carrier absorption is dominant. The carrier concentration of GaP is n ≈ 10 ^{12}cm^{-3}. The THz wave power in the 3.2 – 4.42 THz frequency region decreases rapidly. For frequencies above 4.5THz, the deviation increases considerably because of the dispersion curve of the polariton branch of GaP. The length of the GaP crystal (L) is 10 mm and the beam spot size (ϕ) of NIR lasers on the GaP input surface is 700μm. It is estimated that for the frequency 4.5 THz, the generated THz wave

propagates with an angle $\psi \sim 17.5°$, which is same as the critical angle for total internal reflection in GaP. To generate THz waves above 4.5 THz, we need to rotate the GaP crystal relative to the input lasers to prevent the total internal reflection.
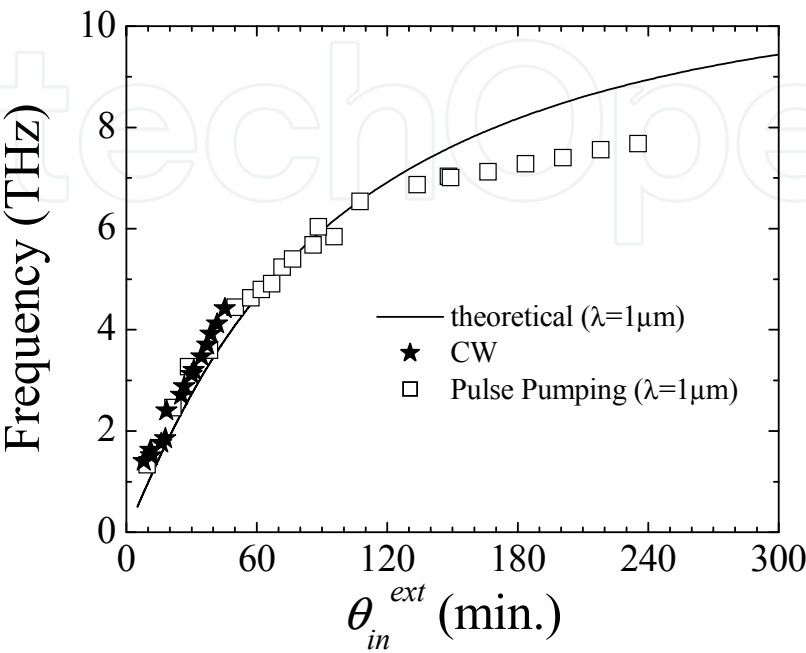

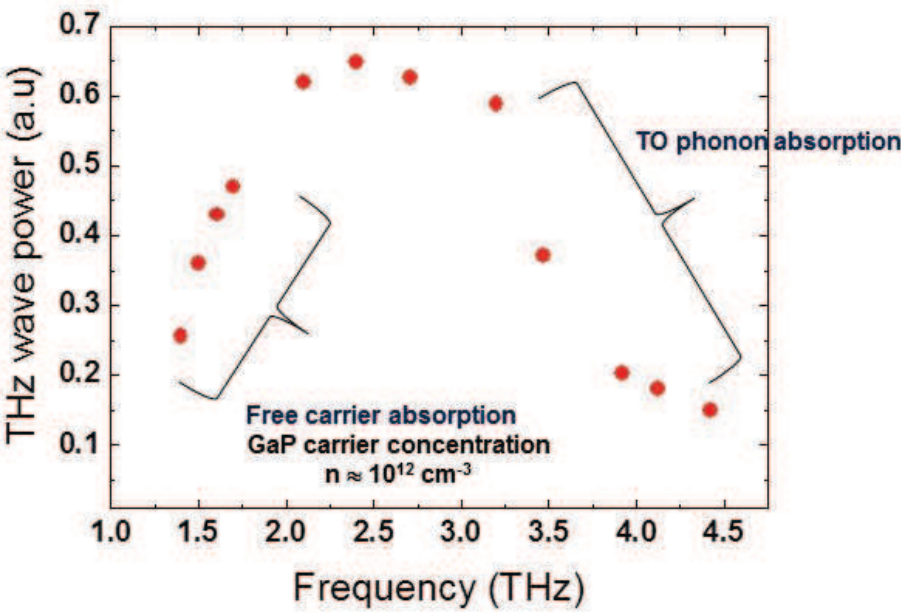Fig. 4. The phase matching angle relation with THz wave frequency.

Fig. 5. The frequency dependence of THz wave maximum output power.

5. Power scaling of the CW THz source

Assume two Gaussian pump beams with the same beam radius and no diffraction effect. The output power of the generated THz waves in DFG can be calculated by using the following formula [30]

$$P_{THz} = \frac{4\ P_1 P_2 \pi^2 d_{eff}^2 L_{eff}^2}{c\epsilon_0 n_1 n_2 n_3 \lambda_1^2 S} \tag{6}$$

where P_1, P_2 are the effective powers of the pump and signal beams. L_{eff} is the effective interaction length of the two near –IR beams inside the crystal (GaP), d_{eff} is the effective nonlinear coefficient, λ_1 is the output wavelength of THz wave, n_1, n_2, and n_3 are the indices of refraction for pump, signal and THz beams respectively, c is the speed of light in vacuum, ϵ_0 is the permittivity constant and S is the cross-sectional area of the pump and signal beams defined by the $1/e^2$ radius of the Gaussian beam. The power density of the two laser diodes are enhance up to 2 W each by employing two ytterbium doped polarization maintained fiber amplifiers (FAs). When the pump power is limited the THz wave power can be improved by (i) employing longer GaP crystal and (ii) decreasing the beam spot size of the near-IR lasers.

5.1 THz wave power dependence with GaP crystal length

We have investigated the THz wave output power dependence on GaP crystal length. THz waves are generated using 2.5, 5, 10, 15 and 20 mm long GaP crystals over the frequency range from 1.5 – 3 THz as θ_{in}^{ext} is varied from 9′ to 23.6 ′. The bandwidth for half the maximum power was about 600 GHz when the θ_{in}^{ext} is fixed. Generated THz waves are detected with a calibrated Si bolometer. The beam spot size (ϕ) of the pump and signal beams are 700 μm. Fig. 6(b), shows the theoretically predicted THz wave output power behavior against the GaP crystal length at frequencies 1.5, 2 and 3 THz respectively. In estimating the THz wave power, we taken into account of the effective interaction length (L_{eff}) of the two NIR beams in non-collinear configuration and also the THz wave absorption effects in GaP crystal at each frequency. The experimental data of THz wave power with GaP crystal length for frequencies 1.5,2 and 3 THz is shown in fig. 6(a), and it is seen that for frequencies 1.5 and 2 THz, the THz power is increased with 2.5 - 20 mm long crystals as expected from the theory. The THz wave power is not saturated even for 20 mm long GaP crystal. But for frequency 3 THz, the THz wave power increased for 2.5- 10 mm long GaP crystals and decreased with 15 and 20 mm long crystals. This behavior is clearly agrees with the theoretical prediction as shown in the fig. 6(b).

The reasons may be the power losses due to absorption effect in GaP are not dominant even for 20 mm long crystal at 1.5 and 2 THz in the lower the frequency region, however at higher frequencies (above 2.5 THz) the THz absorption effects in longer crystals may not be negligible in GaP crystal [31]. The THz power is expected with proportional to the square of the effective crystal length L_{eff}. Here L_{eff} represents the effective interaction length of the NIR beams in non-collinear phase-matched mixing and is given by

$$L_{eff} = \left(\frac{L\phi}{\sin\psi} \right)^{1/2} \tag{7}$$

Where L is length of GaP crystal, ϕ is beam spot size of the input laser beam, ψ is angle of generated THz wave inside GaP relative to the pump beam as shown in fig. 2(b).

The fig. 7 indicates that the advantage of using a longer crystal is not applicable at higher frequencies (above 2.5 THz) due to the THz wave absorption effects in longer GaP crystals.
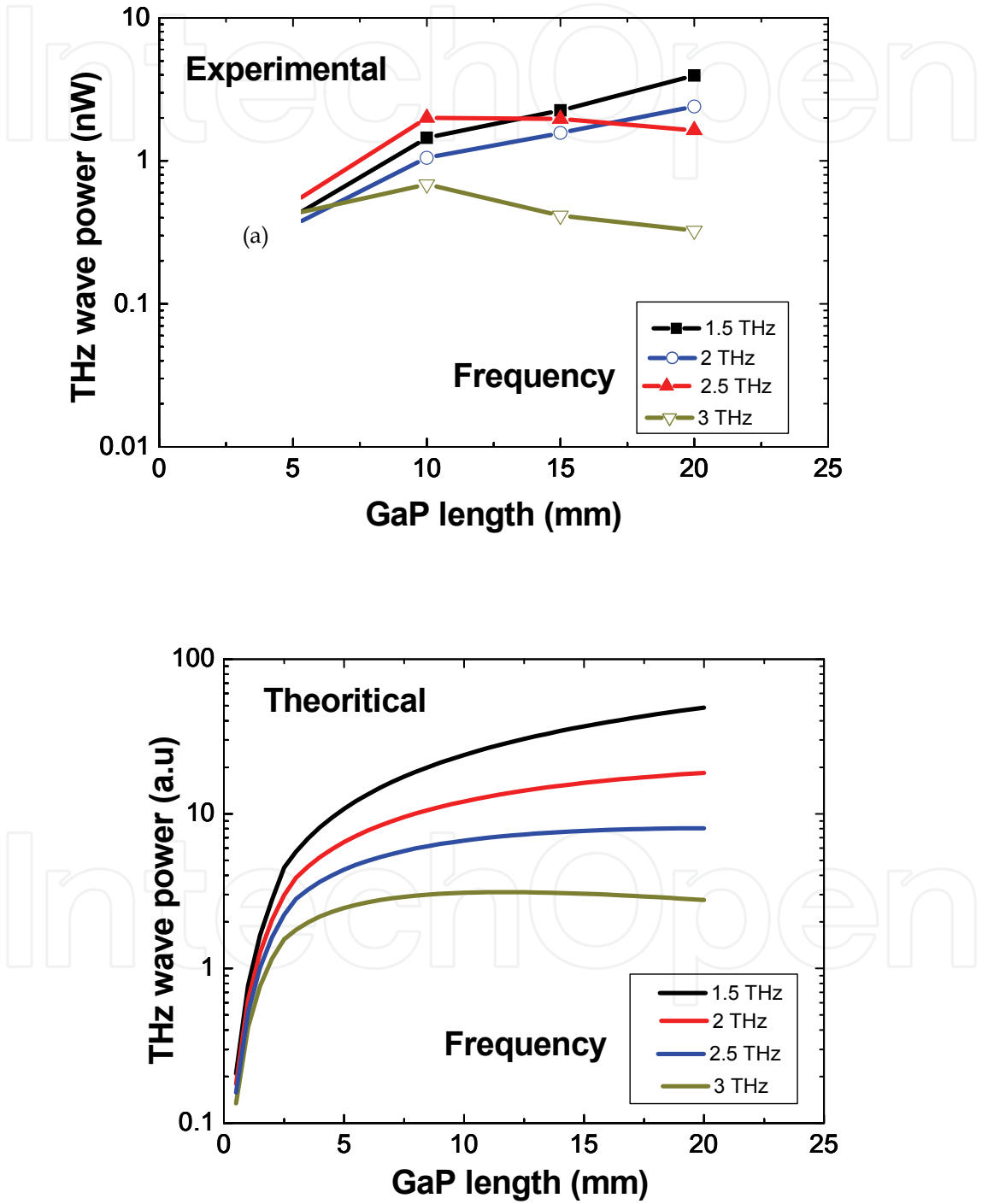

Fig. 6. (a) THz wave power dependence on GaP crystal length at 1.5-3 THz.
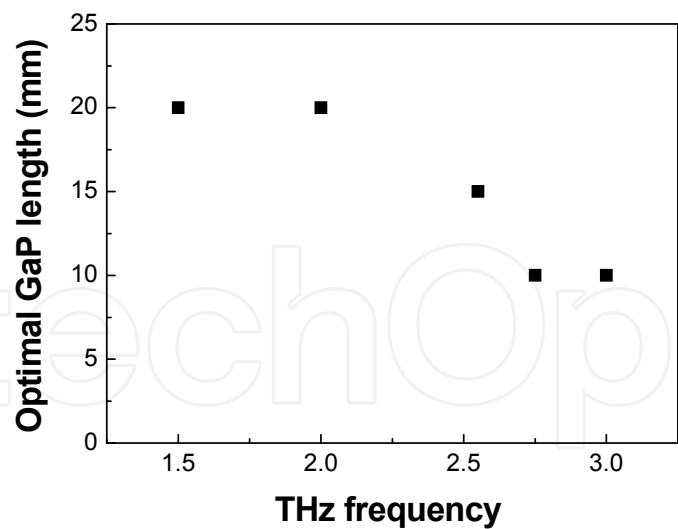(b) The theoretical behavior.

Fig. 7. The optimal GaP crystal length for THz wave frequency to obtain the maximum power.

5.2 THz wave power dependence with beam spot size of pump and signal lasers

The THz wave power is inversely proportional to the spatial overlap of cross-sectional areas of pump and signal lasers, and hence the enhancement of output power is possible by decreasing the beam spot size of the pump and signal lasers. We have investigated the THz wave power dependence for various beam spot sizes (1.2 mm-300 µm) of input near-IR lasers at a frequency of 1.62 THz using a 10 mm long GaP crystal. Focal lengths of 600 – 150 mm were used to achieve the beam spot sizes of 1.2 mm – 300 µm. A polyethylene lens with a diameter 2.5 cm was used to collect the THz waves in this configuration. It is seen from fig. 8(a) that THz wave power sharply increased as the beam spot size was reduced from 1.2 mm–500 µm.
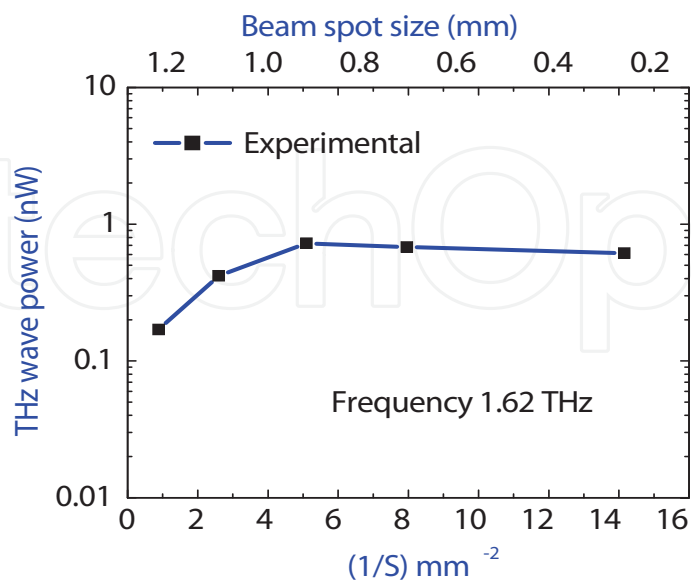

Fig. 8. (a) The THz wave power dependence on the inverse of spatial overlapping of cross-sectional areas of pump and signal lasers at 1.62 THz.
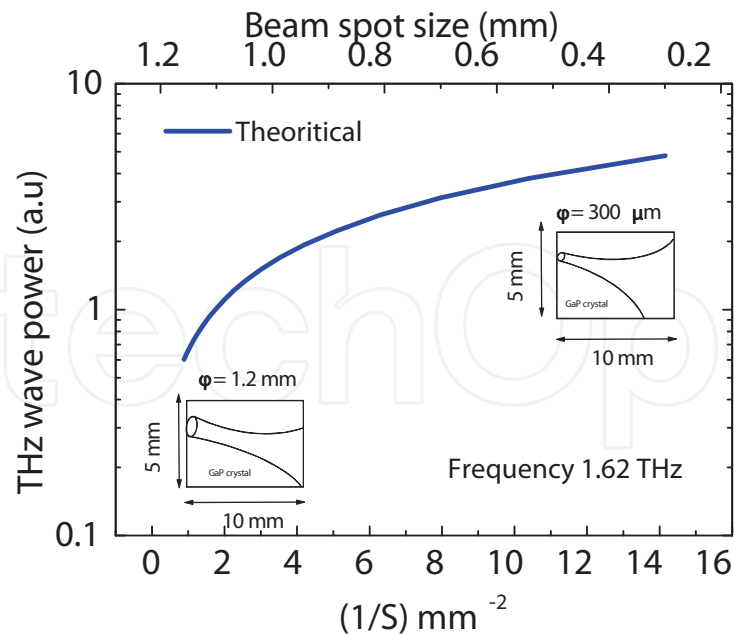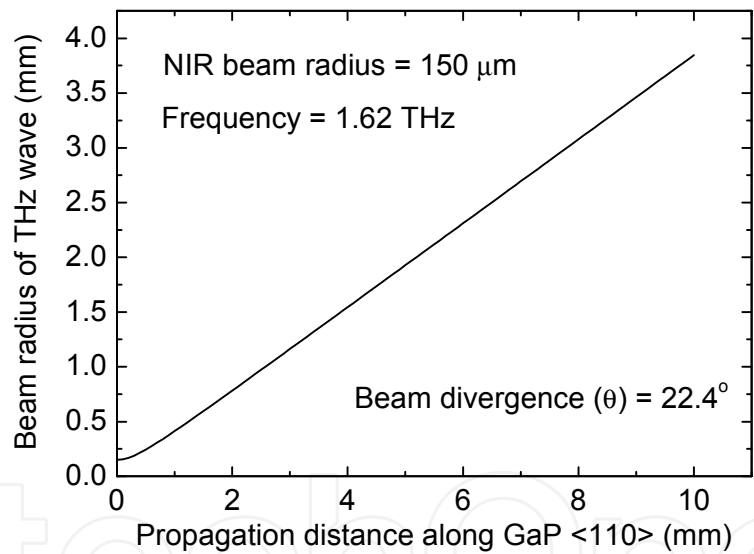
Fig. 8. (b) The theoretical behavior.

Fig. 9. The THz wave divergence inside the GaP crystal along <110> direction for the near-IR beam spot size 300 µm.

This behavior agrees with the theoretical calculation as shown in the Fig. 8(b). However, for beams spot sizes of 400 µm and 300 µm, the THz power was decreased. The output power discrepancy between the experimental data and theory in this region may have been caused by the divergence effect of the THz waves. Thus, in order to under-stand the reason for power decrement, the THz wave divergence effect at beam spot sizes of 1.2 mm and 300 µm was considered.The beam divergence of THz wave was estimated to be ~ 5.6° and ~ 22. 4° for near-IR beam spot sizes of 1.2 mm and 300 µm, respectively. Fig. 9 shows the THz wave divergence inside the GaP crystal along <110> direction for the near-IR beam spot size 300 µm. This shows that the beam divergence of THz wave was very dominant for near-IR beam spot sizes of 300 µm, as the beam spot size is of the same order as that of the wavelength of

the generated THz waves. Another reason for reduction of the THz power in this region (500- 300 μm) may be that the effective interaction length L_{eff} is increases as square root of beam spot size for a given value of crystal length. Fig. 10. shows the dependence of L_{eff} on beam spot size of input lasers. It is seen that for the near-IR beam spot sizes below 400 μm, the effective interaction length is less than 4 mm and THz beam divergence is very significant. So in order to achieve high-power, one has to consider effects of beam divergence, the effective interaction length of the NIR beams, and also the absorption in the crystal. It is known that the GaP lattice absorption is dominant in the high frequency region (above 2.5 THz), and also effective interaction length is increases with beam spot size of NIR lasers. Therefore it is very important to select these parameters (frequency, crystal length, beam spot size) in order to improve the THz wave power.
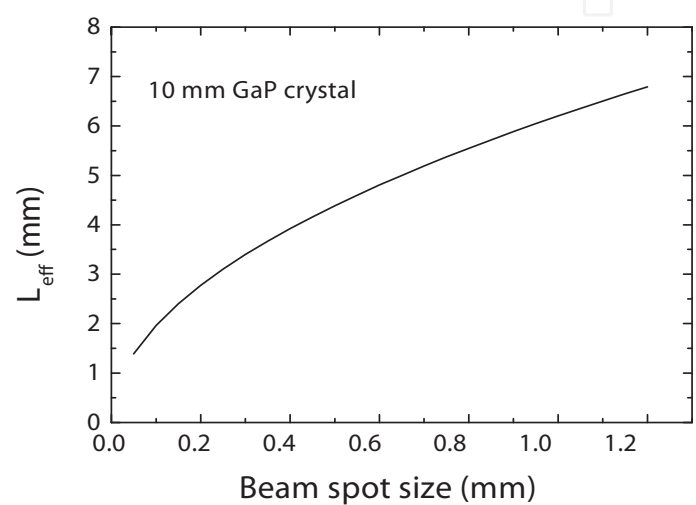

Fig. 10. The dependence of L_{eff} on beam spot size of input lasers.

6. Applications

We constructed a high resolution terahertz (THz) spectroscopic system with an automatic scanning control using our CW THz wave source 11(a). The wavelength of DFB laser was automatically tuned from 1058-1061 nm with a line width of 3 MHz by changing the temperature of the laser.
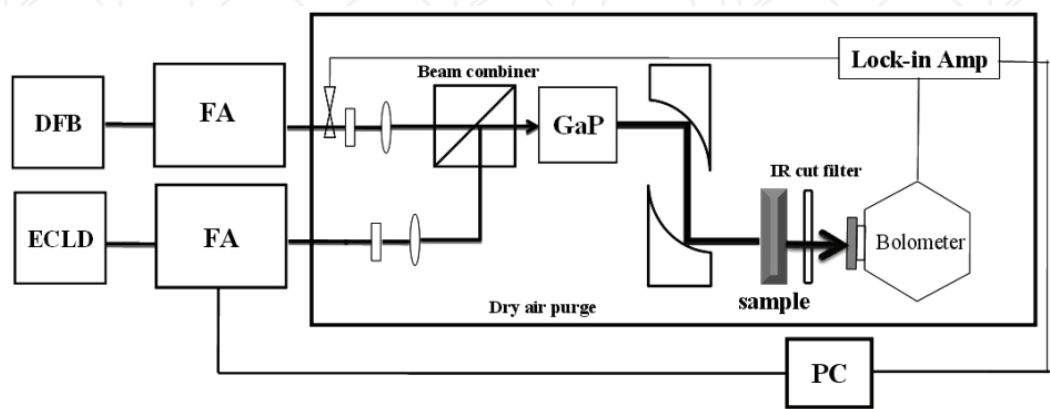

Fig. 11. (a) Schematic diagram of automatic measurement system of cw THz wave spectrometer using GaP.

The wavelength of the ECLD was manually tuned from 1020 nm - 1080 nm with a line width of 4 MHz. Two polarization maintained (PM) ytterbium doped FAs were used to separately amplify the output power of each laser diode up to 2 W. Using micro lenses with focal lengths of 8.5 mm, the amplified laser beam from each FA was collimated to a diameter of 3 mm with a circular shapeA very small angle between the two near-IR beams was required for the DFG to satisfy the non-collinear phase matching condition [22]. The phase-matching condition is fulfilled automatically by rotating and linearly translating the cubic polarizer with a PC controller via GPIB interface using visual basic software. Thus, an efficient spatial overlap of near-IR laser beams was automatically realized on the input surface of a GaP crystal at any beam angle. The near-IR beam spot size is focused to 700µm on the GaP input surface by using lenses with focal lengths of 500 mm. GaP crystals of 10 mm and 15 mm long were cut into a rectangular shape, its length being in the <110> direction and its thickness being in the <001> direction. These parameters such as beam spot size and crystal length are very important to obtain the improved THz wave power [23].
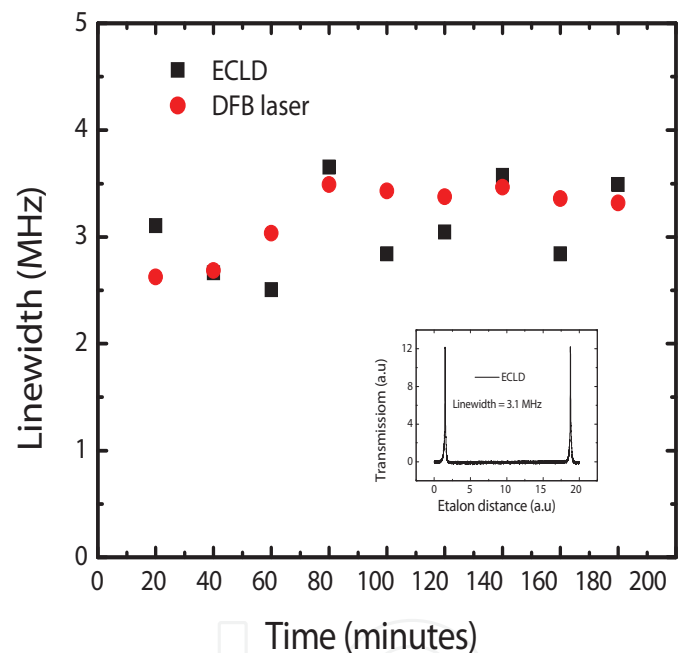

Fig. 11. (b) Frequency stability of DFB and ECLD lasers.

Both the input and output faces of crystal were coated with Al_2O_3, using EB-evaporation after mechanical polishing and chemical etching. The polarizations of the pump and signal beams were adjusted in the <001> and <110> directions, respectively. The frequency stability of diode lasers was measured with Fabry-Perot interferometer in confocal configuration for duration of 3 hours at room temperature (298 K). Figure 11(b) shows the frequency stability of DFB and ECLD lasers and the inset shows interference pattern of the ECLD laser. The linewidth of the diode lasers was calculated by the following formula:

$$Linewidth \quad = \quad \left(\frac{\text{FWHM of the interference wave}}{\text{Distance between the Interference peaks}} \right) \times free\,spectral\,range \qquad (8)$$

The free spectral range (FSR) of the etalon was 2 GHz. The calculated linewidth of ECLD for full width at half maximum (FWHM) was ranging from 4 ~ 8 MHz and that of DFB laser was 4 ~ 7 MHz, respectively for the duration of 3 hours. Note that the linewidth is sensitive and depends on the conditions such as acoustic noise and thermal vibrations. That the spectral distribution of the diode lasers was well described with Gaussian function. Then, in order to know the frequency resolution of THz spectrometer, we can well estimate the linewidth of diode laser by full width at quarter maximum (FWQM). The FWQM linewidth of the ECLD was 2.5 ~ 4 MHz and that of DFB laser was 2.5 ~ 3.5 MHz, respectively. Thus it is concluded that the estimated linewidth of the THz wave for FWQM was < 8 MHz. The centre frequency fluctuation of the diode lasers were within 4 MHz and thus the frequency drift of generated THz waves were estimated to be within 8 MHz. The generated CW THz waves were collected by a pair of off-axis parabolic reflectors and detected with a Si bolometer, cooled to 4.2 K. The Si-bolometer was calibrated with a black body source at 350° C. Black polyethylene film was used to filter out near-IR radiation. The THz wave signal was measured with lock-in amplifier. It is known that the THz wave power stability is dependant on the input diode lasers power stability and overlapping efficiency of the two near-IR beams. A transmission spectrum of water vapor from 1.5- 3 THz was measured. Water vapor is one of the main atmospheric constituents, especially near the earth surface. The THz wave power spectrum was measured and the resonance frequencies of the water vapor were observed in the frequency range from 2 THz to 2.5 THz under room temperature (298 K) and atmospheric pressure conditions by automatically tuning the DFB laser temperature at a fixed phase-matching angle. The wavelength of the DFB laser was tuned from 1058.246–10560.043 nm by changing the temperature of DFB laser diode from 10 - 39.6 C deg. Figure 12(a) shows the water vapor transmission spectrum of THz wave. It is seen that several water vapor absorption lines occur at THz resonance frequencies with FWHM of a few GHz order and every single line of water vapor absorption can be clearly resolved. The thick lines indicate the data from NASA data base [32]. Determining the THz frequency by measuring the wavelength of the pump and signal beams is not sufficiently accurate. The THz frequency was calibrated by using the resonance frequencies of water vapor absorption lines.

We also measured the absorption spectrum of white polyethylene (PE) in the frequency range from 1.97-2.45 THz under room temperature (298 K) and atmospheric pressure conditions. Dry air is purged to eliminate the water vapor absorption in the path of the THz wave. The spectral peak at 70 cm^{-1} (2.1 THz) is known as B_{1u} translation lattice vibration mode of the orthorhombic polyethylene crystal [33]. Such low frequency lattice vibration arises from weak H·H atom interactions forming a PE crystal lattice. The PE sample has dimensions of 5 mm thickness, 10 mm width 15 mm long. The Si- bolometer window contains an edge type white polyethylene. The dimensions of the wedge on the poly window are, the thick side is 2.032 mm and the thin side is about 0.762 mm. So in order to accurately obtain the absorption coefficient of PE sample, we considered the absorption of the wedge type polyethylene window inside the Si-bolometer. We measured the absorption spectrum of wedge on poly of the bolometer by using a pulsed THz wave spectrometer system based on pumping with Cr: forsterite lasers.
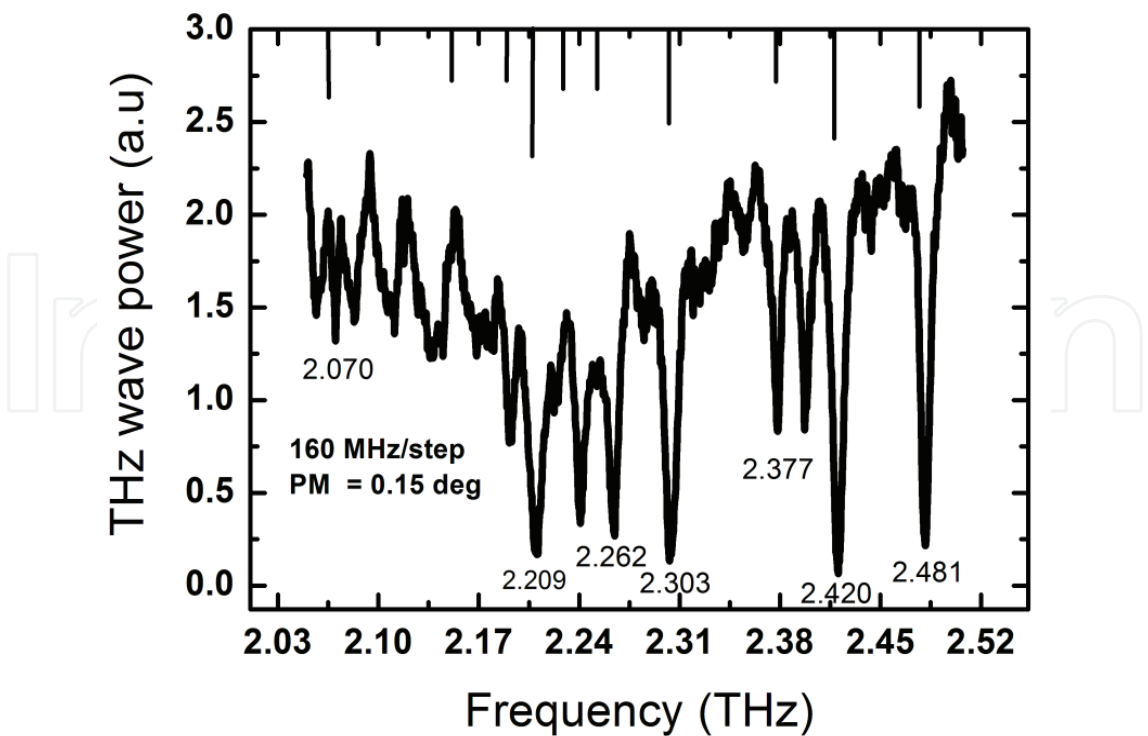
Fig. 12. (a) The CWTHz wave power spectrum with water vapor absorption lines.
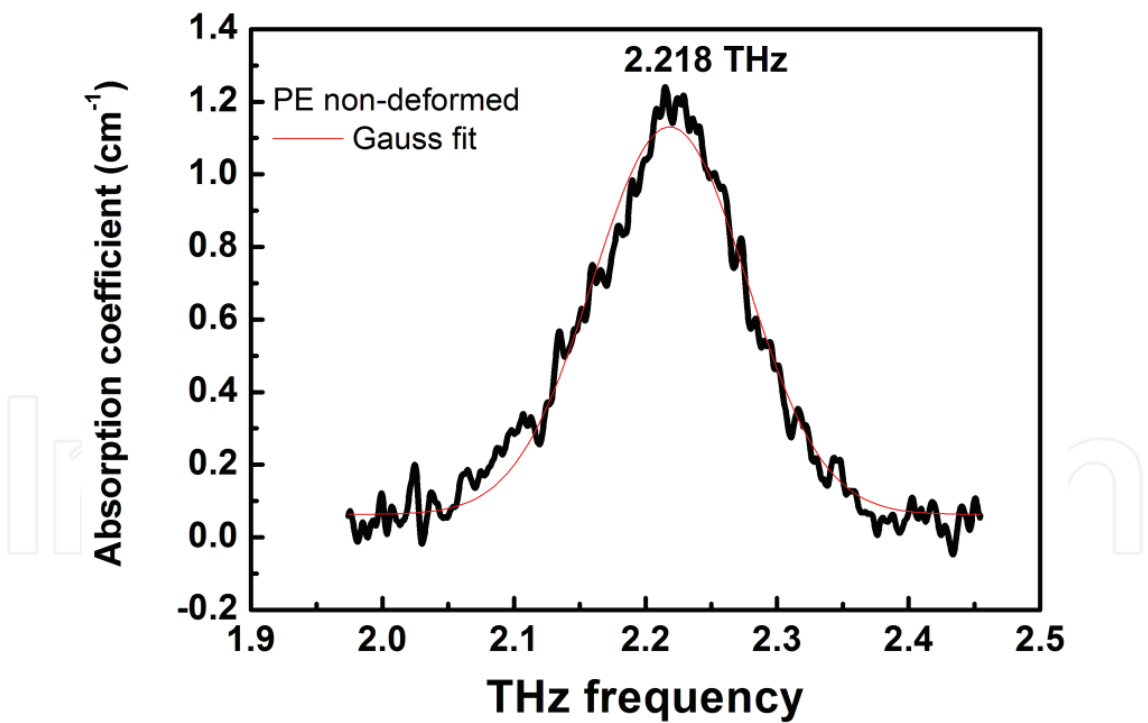

Fig. 12. (b) The absorption spectrum of white PE in the frequency of 1.97– 2.45 THz.

Figure 12(b) shows the absorption spectrum of white polyethylene in the frequency from 1.97-2.45 THz. The data analysis was done by cancelling the absorption effect of the wedge type polyethylene window inside the Si-bolometer. The B_{1u} translation vibration mode of white PE is resolved to be 2.203 THz. Note that the linewidth of the THz wave source

estimated to be < 8 MHz. The B_{1u} vibration mode of the PE is very sensitive to the deformation direction. It is shown that the polarization THz measurements are helpful for non-destructive diagnosis of polymer chains in deformed ultra-high molecular weight polyethylene (UHMWPE) [34]. This CW THz spectrometer has potential application to precisely resolve the vibration mode of the PE crystals with respect to the crystal deformation. Also, this narrow linewidth frequency tunable THz wave source has potential applications in high resolution spectroscopy for investigating resonance properties of various materials.

7. Conclusion

Continuous-wave (CW) and frequency tunable coherent THz radiation was successfully generated at room temperature based on laser diode pumping via excitation of phonon-polariton in GaP crystal. The pump and signal laser sources were an ECLD and a DFG lasers. A two fiber amplifier system was implemented to separately amplify the optical power of the pump and signal lasers respectively. Two methods to improve the generated THz wave output power was proposed and investigated. In order to achieve improved output power, the effects of beam divergence, the effective interaction length in non-collinear mixing and also the absorption in the nonlinear optical crystal must be considered. A high resolution terahertz (THz) spectroscopic system with an automatic scanning control using the CW THz wave generator was constructed. The frequency of THz waves was tuned automatically by changing the temperature of the DFB laser using a system control. The power and frequency stability of the diode lasers were studied. The water vapor transmission characteristics of the THz wave and also absorption spectrum of white polyethylene were investigated. The advantage of our CW THz wave system is its very wide frequency tunability with narrow line width and it has potential applications in high resolution spectroscopy.
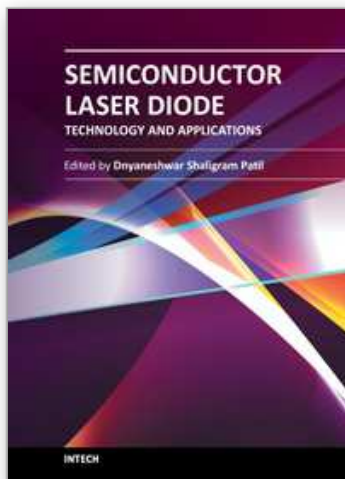
8. Acknowledgements

9. References

[1] Nishizawa.J (1963), History and characteristics of semiconductor laser, *Denshi Kagaku*, vol.14, pp.17-31, 1963.

[2] Nishizawa.J (1965), Esaki diode and long wavelength laser, *Denshi Gijutu,* vol. 7, pp.–106, 1965.

[3] Nishizawa.J (1957), Semiconductor Maser, *Japan patent 273217*, Apr.1957.

[4] Nishizawa.J & Suto.K (1980), Semiconductor Raman laser, *J.Appl.Phys*, vol. 51, pp.2429-2431, 1980.

[5] Suto.K, Nishizawa.J (1983), Low threshold semiconductor Raman laser, *IEEE J.Quantum Electron,* vol.19, pp. 1251-1254, 1983.

[6] Tanabe. T., Suto.K, Nishizawa. J, Saito. K & Kimura. T (2003),Tunable terahertz wave generation in the 3- to 7-THz region from GaP, *Appl.Phys.Lett.,* vol. 83, pp. 237- 239, 2003.

[7] Auston. H, Cheung. K.P. & Smith. P.R. (1984), Picosecond photoconducting Hertzian dipoles, *Appl.Phys.Lett.,* vol. 45, pp. 284-286, 1984.

[8] Fattinger. Ch. & Grischkowsky. Ch. (1988), Point source terahertz optics, *Appl. Phys.Lett.,* vol.53, pp.1480-1482, 1988.

[9] Hu. B. B., Darrow. J. T, Zhang. X-C, Auston. D. H & Smith. P. R (1990), Optically steerable photoconducting antennas, *Appl.Phys.Lett.,* vol. 56, pp. 886-888,+ 1990.

[10] Xu. L., Zhang. X-C & Auston. D. H. (1992), Terahertz beam generation by femto optical pulses in electro optic materials, *Appl.Phys.Lett.,* vol. 61, pp. 1784-1786,1992.

[11] Karpowicz. N, Zhong. H., Jingzhou. X, Lin. K-I., Hwang. J-S & Zhang. X-C. (2005), Comparison between pulsed terahertz time-domain imaging and continuous terahertz imaging, *Semicond.Sci.-Technol.",* vol. 20, pp. S293-S299, 2005.

[12] Siebert. K.J, Quast. H., Leonhardt. R, Loffler. T., Thomson. M, Bauer. T, Roskos H. Gand Czasch. S (2002), Continuous-wave all optoelectronic terahertz Imaging, *Appl.Phys.Lett.,* vol.8, 3003-3005, 2002.

[13] Kohler. R., Tredicucci. A, Beltram. A, Beere. H. E., Linfield. E.H, Ritchie. A., Iotti. R. C., and. Rossi. F (2002), THz semiconductor hetero structure laser, *Nature,* vol. 417, pp. 156-159, 2002.

[14] Yu. J. S, Slivken. S, Evans. A, Darvish. S. R, Nguyen. J and Razeghi. M (2006), High power λ ~ 9.5 μm quantum- cascade lasers operating above room temperature in continuous-wave mode, *Appl.Phys.Lett.,* vol. 88, pp. 091113, 1-3, 2006.

[15] McIntosh. K.A, Brown. E. R., Nichols. K. B, McMahon. O. B, DiNatale. W. F and Lyszczarz. T. M (1995), Terahertz photomixing with diode lasers in low-Temperature grown GaAs," *Appl.Phys.Lett.,* vol. 67, pp. 3844-3846, 1995.

[16] Kleine-Ostmann. T, Knobloch. P, Koch. M., Hoffmann. S., Breede. M, Hofmann. M, Hein. G, Pierz. K, Sperling. M and Donhuijsen. K (2001), Continuous THz imaging, *Electron.Lett.,* vol. 37, pp.1461-1462, 2001.

[17] Sasaki. Y, Yokoyama. H, and Ito. H (2005), Surface-emitted continuous-wave terahertz using periodically poled lithium niobate, *Electron.Lett.,* vol. 41, pp. 712- 713, 2005.

[18] Baker. C, Gregory. I, Evans. M.,.Tribe. W, Linfield. E. and Missous. M (2005), All optoelectronic terahertz system using low-temperature grown InGaAs photo mixers," *Opt.Express,* vol. 13, pp. 9639- 9644, 2005.

[19] Stone. M. R, Naftaly. N, Miles. R.E, Mayorga I.C, Malcoci. A and Mikulics. M (2005), Generation of continuous-wave terahertz radiation using two-mode sapphire laser containing an intracavity Fabry-Perot etalon,"*J.Appl.Phys.,* vol. 97, pp.103108.1-4, 2005.

[20] Ding. Y.J and Shi. W (2003), Widely-tunable, monochromatic, and high power terahertz and their applications", *Journal of Nonlinear Optical Physics & Materials,* vol. 12, no. 4, pp- 557-585, 2003.

[21] Kawase. K, Shikata. J.-I, Imai. K and Ito. H (2001), *Appl. Phys. Lett.* 78, 2819,2001.

[22] Nishizawa. J, Tanabe. T, Suto. K, Watanabe.Y, .Sasaki. T and Oyama. Y (2006), Continuous-wave frequency tunable Terahertz-wave generation from GaP," *IEEE Photon.Technol. Lett.,* vol.18, no. 19, pp. 2008, 2010, 2006.

[23] Ragam.S, Tanabe.T,. Saito.K, Oyama. Y and Nishizawa. J (2009), Enhancement of CW THz wave power under non-collinear phase-matching conditions in DFG, *Journal of Light wave Technology,* vol.27, no. 15, pp 3057-3061, 2009.

[24] Shi. W and Ding. Y. J(2003), *Appl. Phys. Lett.,* 83, 848, 2003..

[25] Shi. W and Ding. Y. J (2002), *Opt. Lett.,* 27 ,1454, 2002.

[26] Kondo. T and Shoji.I (2005), *IPAP Books,* 2 , 151, 2005.

[27] http://www.clevelandcrystals.com/Default.htm

[28] Tomita. I, Suzuki. H, Ito. H, Takenouchi. H, Ajito. K, Tungsawang. T and Ueno. Y(2006), *Appl. Phys. Lett.,* 88, 071118, 2006.

[29] Bahoura. M., Herman. G. S., Barnes. N. P, Bonner. C. E, and Higgins. P. T (2000), *Proceeding of SPIE,* 3928 132, 2000.

[30] Shen. Y,R (1977), *Nonlinear infrared generation,* page 62, 1977.

[31] Saito. K, Tanabe. T, Oyama. Y, Suto. K, Kimura. K, and Nishizawa. J (2008), Terahertz wave absorption in GaP crystals with different carrier densities," *Journal of Physics and Chemistry of Solids,* 69, pp. 597- 600, 2008,.

[32] http://www.jpl.nasa.gov/

[33] Tasumi M and Shimanouchi T (1965), crystal vibrations and intermolecular forces of polymethylene crystals *J.chem.phys.* vol.43, 1245, 1965.

[34] Ragam.S, Tanabe.T,. Oyama. Y and Watanabe. K (2010), Comparison of CW THz spectrometer developed with laser diode excitation and pulsed THz wave spectrometer with Cr: Forsterite source, *JInfrared, MilliTerahz Waves, 31(10),1164-1170, 2010.*

Semiconductor Laser Diode Technology and Applications

Edited by Dr. Dnyaneshwar Shaligram Patil

This book represents a unique collection of the latest developments in the rapidly developing world of semiconductor laser diode technology and applications. An international group of distinguished contributors have covered particular aspects and the book includes optimization of semiconductor laser diode parameters for fascinating applications. This collection of chapters will be of considerable interest to engineers, scientists, technologists and physicists working in research and development in the field of semiconductor laser diode, as well as to young researchers who are at the beginning of their career.

How to reference

In order to correctly reference this scholarly work, feel free to copy and paste the following:

Srinivasa Ragam (2012). CW THz Wave Generation System with Diode Laser Pumping, Semiconductor Laser Diode Technology and Applications, Dr. Dnyaneshwar Shaligram Patil (Ed.), ISBN: 978-953-51-0549-7, InTech, Available from: http://www.intechopen.com/books/semiconductor-laser-diode-technology-and-applications/cw-thz-wave-generation-system-with-diode-laser-pumping

INTECH
open science | open minds